Molecular Cell, Vol. 7, 263–272, February, 2001, Copyright ©2001 by Cell Press

BRCA2 Is Required for Homology-Directed Repair of Chromosomal Breaks

Mary Ellen Moynahan,*† Andrew J. Pierce,† and Maria Jasin†‡
*Department of Medicine
†Cell Biology Program
Memorial Sloan-Kettering Cancer Center
New York, New York 10021

Summary

The BRCA2 tumor suppressor has been implicated in the maintenance of chromosomal stability through a function in DNA repair. In this report, we examine human and mouse cell lines containing different *BRCA2* mutations for their ability to repair chromosomal breaks by homologous recombination. Using the I-SceI endonuclease to introduce a double-strand break at a specific chromosomal locus, we find that BRCA2 mutant cell lines are recombination deficient, such that homology-directed repair is reduced 6- to >100-fold, depending on the cell line. Thus, BRCA2 is essential for efficient homology-directed repair, presumably in conjunction with the Rad51 recombinase. We propose that impaired homology-directed repair caused by BRCA2 deficiency leads to chromosomal instability and, possibly, tumorigenesis, through lack of repair or misrepair of DNA damage.

Introduction

Germline mutations in either of the breast cancer susceptibility genes *BRCA1* or *BRCA2* predispose to breast, ovarian, and other cancers (Rahman and Stratton, 1998). Inheritance of one defective allele of either gene is sufficient to confer cancer predisposition, but tumors from predisposed individuals consistently exhibit loss of heterozygosity, implying that the *BRCA1* and *BRCA2* gene products act as tumor suppressors. Both genes encode large nuclear proteins whose function in tumor suppression has been a matter of speculation, although roles in both DNA repair and transcription have been ascribed (Welcsh et al., 2000).

Common to BRCA1 and BRCA2 is a physical interaction with the mammalian Rad51 protein, a homolog of bacterial RecA that catalyzes strand exchange during homologous recombination (Cox, 1999). Both proteins colocalize with Rad51 to nuclear foci after DNA damage and at forming synaptonemal complexes early in meiotic prophase (Scully et al., 1997; Chen et al., 1998a). The interaction of BRCA2 with Rad51 is mediated by a series of internal BRC repeats (Wong et al., 1997; Chen et al., 1998b), with an additional Rad51-interacting domain described for mouse Brca2 at the extreme C terminus (Mizuta et al., 1997; Sharan et al., 1997). Consistent with a role for these proteins in DNA repair, BRCA1- and BRCA2-deficient mouse and human cells display chromosome instability and are sensitive to DNA-damaging agents, particularly those agents that cause DNA double-strand breaks (DSBs; Connor et al., 1997; Sharan et al., 1997; Chen et al., 1998b; Gowen et al., 1998; Patel et al., 1998; Shen et al., 1998; Abbott et al., 1999).

Homologous recombination is a conserved pathway for the repair of DSBs, with Rad51 postulated to play a central role (Cox, 1999; Pâques and Haber, 1999). In mammals, as in other organisms, homology-directed repair (HDR) of a DSB maintains genomic integrity through precise repair by gene conversion, using the sister chromatid as a repair template (Johnson and Jasin, 2000). Nonhomologous repair mechanisms also play a major role in the repair of DSBs in mammalian cells, although this type of repair is generally thought to be imprecise and potentially more mutagenic (Jeggo, 1998). BRCA1-deficient cells have recently been demonstrated to have impaired HDR of a chromosomal DSB, whereas nonhomologous repair was not diminished (Moynahan et al., 1999). A similar role for BRCA2 as a caretaker of genomic stability would suggest that BRCA2 inactivation could foster tumorigenesis by increasing the likelihood that cells would accrue mutations in genes that control cell division, death, or life span.

In this study, we sought to directly determine whether BRCA2 plays a role in homologous repair of DSBs by examining the repair of a DSB introduced into a defined site in the genome. We report that human and murine cells carrying different *BRCA2* mutations have a diminished capacity to repair a chromosomal DSB by gene conversion. These findings establish a biological function for BRCA2 that is relevant to carcinogenesis.

Results

BRCA2-Deficient CAPAN-1 Cells Are Defective in HDR

The human pancreatic adenocarcinoma cell line, CAPAN-1, carries a 6174delT mutation on one allele of *BRCA2* with loss of the wild-type *BRCA2* allele (Goggins et al., 1996). This frameshift mutation, which is frequent in families with hereditary breast and ovarian cancer, leads to a truncation after amino acid 1981 within BRC repeat 7 (Figure 1A). Consistent with this, the CAPAN-1 cell line has been demonstrated to express a truncated BRCA2 protein (Marmorstein et al., 1998; Su et al., 1998).

This cell line was reported to be hypersensitive to genotoxic agents specifically capable of producing DNA DSBs (Abbott et al., 1998; Chen et al., 1998b). To test whether the hypersensitivity is due to impaired HDR of chromosomal DSBs, we introduced a recombination repair substrate into the CAPAN-1 genome (Figure 2). The repair substrate incorporates a direct repeat green fluorescent protein (DR-GFP) reporter, and assays noncrossover gene conversion events (Pierce et al., 1999). DR-GFP is composed of two differentially mutated green fluorescent protein (GFP) genes (Figure 2A). The *SceGFP* gene is a mutated GFP gene that contains the 18 bp recognition site for the rare cutting I-SceI endonuclease,

‡To whom correspondence should be addressed (e-mail: m-jasin@ski.mskcc.org).

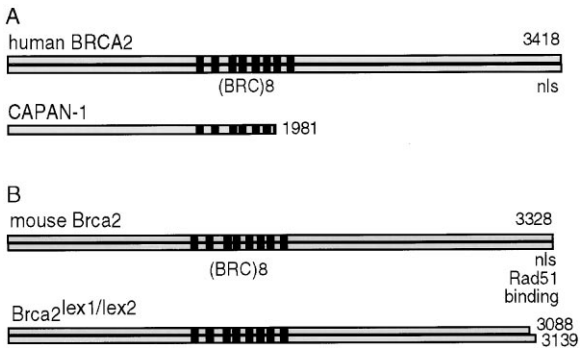

Figure 1. Schematic of Wild-Type and Mutant BRCA2 Proteins

(A) Human BRCA2 protein is 3418 amino acids long. Notable structural motifs include a centrally located region of eight BRC repeats (black bars) that interacts with Rad51 and a C-terminal nuclear localization signal (nls). In the CAPAN-1 pancreatic cancer cell line, one *BRCA2* allele contains a 6174delT mutation and the other allele is lost. The mutant *BRCA2* allele encodes a truncated protein of 2002 amino acids, including 1981 BRCA2 amino acids and 21 amino acids that are generated by the frameshift. The truncation of BRCA2 sequences at amino acid 1981 occurs within BRC repeat 7.

(B) The murine Brca2 protein is 3328 amino acids long, and is 59% identical to human BRCA2, although specific regions are highly conserved (Sharan and Bradley, 1997). Conserved regions include the centrally located BRC repeats and the nls (amino acids 3189–3238). An additional Rad51-interacting domain was identified at the same region in the C terminus of the murine protein as the nls (amino acids 3196–3232). *Brca2*$^{lex1/lex2}$ ES cells harbor two different alleles, both of which encode truncated Brca2 proteins deleted for the C-terminal Rad51-interacting domain and the conserved nls identified by sequence homology.

and as a result will undergo a DSB when I-SceI is expressed in vivo. The I-SceI site was incorporated at a BcgI restriction site by substituting 11 bp of wild-type GFP sequences with those of the I-SceI site. These substituted base pairs also introduce two in-frame stop codons. Downstream of *SceGFP* is an 812 bp internal GFP fragment *(iGFP)* that can be used to correct the mutation in the *SceGFP* gene to result in a *GFP*+ gene. Molecular analysis has previously confirmed that GFP-positive cells following I-SceI expression are derived from a noncrossover gene conversion within the DR-GFP substrate (Pierce et al., 1999). By contrast, deletional recombinational events give rise to a 3′-truncated GFP gene that has been shown to be nonfunctional for GFP expression (Pierce et al., 1999). The two GFP genes are separated by a puromycin resistance gene that is used to select for integration of the DR-GFP substrate into the genome of cells.

The DR-GFP substrate was electroporated into CAPAN-1 cells, and clones that had randomly integrated the substrate into the genome were selected with puromycin. Six independently isolated clones were identified by Southern analysis to have undergone integration of an intact, single copy DR-GFP substrate (+, Figure 2B; data not shown). Multiple digests were performed to confirm that the integrated recombination substrate was a single copy, and that no gross changes in the integrity of the reporter substrate had occurred prior to integration (data not shown).

To detect HDR of an induced chromosomal DSB, the I-SceI expression vector pCBASce was transiently transfected into five of the CAPAN-1 DR-GFP clones, and flow cytometry was used to quantify GFP-positive cells (Figure 2C). Due to the slow growth characteristics of CAPAN-1 cells, flow cytometry was performed at different time points to determine the time after transfection for maximal detection of GFP-positive cells. A few GFP-positive cells (0.0086%) were detected maximally 5 days after transfection of pCBASce (Figure 2C; Table 1; data not shown). No GFP-positive cells (or only extremely rare ones) were detected following transfection with negative control DNA, indicating that spontaneous intrachromosomal gene conversion was rare, and that the few GFP-positive cells from I-SceI expression were from DSB-induced recombination. Combining data from the five CAPAN-1 clones, the I-SceI-generated DSB induced HDR approximately 20-fold. This induction of HDR is significantly less than we have typically found in other cell lines with this recombination reporter (Pierce et al., 1999). We attempted to complement the CAPAN-1 cell line by expressing full-length BRCA2 from a cDNA expression vector (Marmorstein et al., 1998). However, we have thus far been unable to detect appreciable expression levels, presumably due to difficulties in expressing this large protein.

To verify that the low frequency of HDR is not due to poor transfection efficiency, the CAPAN-1 clones were also electroporated with the pNZE-CAG vector, which expresses wild-type GFP protein from the same control elements as I-SceI in the pCBASce vector. Maximal GFP expression was detected 3 days after electroporation at a frequency of 12% of the electroporated cells (data not shown), and then declined 5 days after transfection to an average of 4% (Table 1). We can surmise, therefore, that HDR is occurring in approximately 1 per 1400 cells successfully transfected with the I-SceI expression vector, based on a 12% transfection efficiency and an average frequency of recombination of 0.0086%.

We have typically found that a DSB introduced into the genome of rodent cells within the DR-GFP substrate leads to as much as a three order-of-magnitude induction of homologous recombination (Pierce et al., 1999). More recently, we have tested a variety of immortalized human cell lines for HDR and found a similarly large induction of gene conversion, such that recombinants are at least 5% to 10% of the electroporated cells (our unpublished data). With this large induction, recombination is estimated to occur in roughly 1 in 10 cells successfully transfected with the I-SceI expression vector. Thus, the CAPAN-1 cells have more than a 100-fold reduction in homologous repair as compared with other cell lines.

Gene Targeting Is Reduced in *Brca2*$^{lex1/lex2}$ Mouse ES Cells

Due to difficulties in complementing the BRCA2 defect in CAPAN-1 cells as well as the inherent questions raised when analyzing the functional role of gene products in tumor-derived cell lines, we examined the role of BRCA2 in a more genetically defined system. For this, we used murine embryonic stem (ES) cells containing hypomorphic *Brca2* alleles. In addition to the conserved internal BRC repeats, a second Rad51-interacting domain was identified at the C terminus of the mouse Brca2 protein

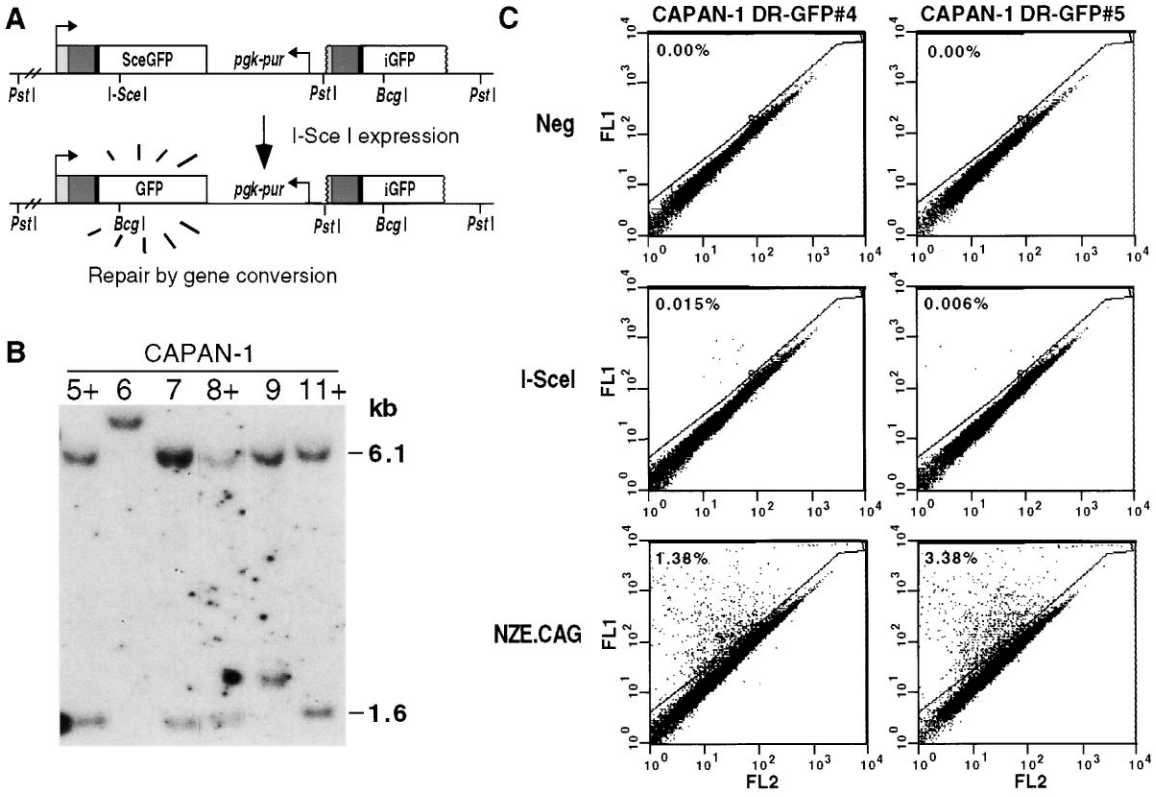

Figure 2. HDR of an Induced DSB in CAPAN-1 Cells Is Defective

(A) The recombination repair substrate DR-GFP is composed of two differentially mutated GFP genes, *SceGFP* and *iGFP.* When I-SceI endonuclease is expressed in cells containing the DR-GFP substrate in their genome, a DSB will be introduced at the I-SceI site in the *SceGFP* gene. Repair of the DSB by a noncrossover gene conversion with the downstream *iGFP* gene results in reconstitution of a functional GFP gene, involving loss of the I-SceI site and gain of the BcgI site. Because the I-SceI site mutation in the *SceGFP* gene entails 11 bp changes including the introduction of two stop codons, homologous recombination between *SceGFP* and *iGFP* is necessary to restore a functional GFP gene (Pierce et al., 1999). The *SceGFP* gene is expressed from the chicken β-actin promoter with cytomegalovirus enhancer sequences. The shaded regions indicate that *SceGFP* and the corrected GFP genes encode an EGFP protein (mutated or wild-type, respectively) fused to a nuclear localization signal (light shading) and zinc finger domain (dark shading) to aid in nuclear retention of the protein (Pierce et al., 1999).

(B) Southern blot analysis of CAPAN-1 clones derived from electroporation of the DR-GFP substrate. Genomic DNA from puromycin-resistant clones was digested with PstI and probed with a radiolabeled GFP fragment. Intact integration of the DR-GFP substrate gives 6.1 and 1.6 kb fragments containing the *SceGFP* and *iGFP* genes, respectively. CAPAN-1 clones 5, 8, and 11 contain the expected fragments from PstI and other restriction analyses, as do clones 4 and 23 (data not shown).

(C) Representative flow cytometric analyses of CAPAN-1 DR-GFP clones to detect cellular green fluorescence following DSB induction. Panels depict clones 4 and 5 following transfection with negative control DNA (top panels), the I-SceI expression vector pCBASce (middle panels), and the GFP expression vector pNZE-CAG (bottom panels). Two-color fluorescence analysis was performed, with the percentage of green fluorescent cells above the diagonal indicated. In each panel, 50,000 cells were analyzed. Flow cytometry shown here was performed 5 days after transfection. FL1, green fluorescence; FL2, orange fluorescence.

by two-hybrid analysis (Mizuta et al., 1997; Sharan et al., 1997). Consecutive gene targeting with two different vectors was performed in ES cells to create a cell line in which both alleles are deleted for this interacting domain, which is encoded by exon 27 (Morimatsu et al., 1998). In the *lex1* allele, only sequences encoded by exon 27 of *Brca2* were deleted, whereas in the *lex2* allele, sequences from exon 27 and part of exon 26 of *Brca2* were deleted (Figure 1B). Although the internal BRC repeats are not perturbed in the $Brca2^{lex}$ alleles, $Brca2^{lex1/lex2}$ cells are hypersensitive to ionizing radiation, indicating a functional significance for the extreme C terminus of the protein (Morimatsu et al., 1998).

We first performed gene targeting assays with the $Brca2^{lex1/lex2}$ ES cells to determine their ability to homologously integrate transfected DNA. Although the precise relationship between gene targeting and HDR has not been established, cell lines with defects in HDR have also been shown to have gene-targeting defects (Essers et al., 1997; Moynahan et al., 1999; Dronkert et al., 2000). To analyze gene targeting, we constructed a vector that incorporates the DR-GFP recombination substrate. In this way, HDR at a defined genetic locus could subsequently be assayed in the gene-targeted clones. The DR-GFP substrate was subcloned in both orientations into a gene-targeting vector for the *pim1* locus on chromosome 17 (te Riele et al., 1990), creating the p59xDR-GFP vectors (see Figure 3A). In these vectors, the selectable hygromycin resistance gene (hyg^R)–coding sequences are fused in-frame to *pim1*-coding sequences, such that

Table 1. CAPAN-1 Cells Exhibit Low Levels of Homologous DSB Repair

CAPAN-1 Clone	Number of GFP-Positive Cells		
	Negative	pCBASce	pNZE-CAG
#4	$<1 \times 10^{-5}$	1.5×10^{-4}	2.9×10^{-2}
#5	$<1 \times 10^{-5}$	0.6×10^{-4}	4.8×10^{-2}
#8	$<1 \times 10^{-5}$	0.3×10^{-4}	3.5×10^{-2}
#11	1×10^{-5}	1.0×10^{-4}	ND
#23	1×10^{-5}	0.9×10^{-4}	ND
All clones	0.4×10^{-5} ($\pm 0.5 \times 10^{-5}$)	0.86×10^{-4} ($\pm 0.45 \times 10^{-4}$)	3.7×10^{-2} ($\pm 1.0 \times 10^{-2}$)

CAPAN-1 DR-GFP cells were transfected with negative DNA, pCBASce, and pNZE-CAG. FACS analysis was performed at 5 days posttransfection. Numbers for each clone are from the average of two or three experiments per cell clone, with 50,000 cells analyzed per experiment. GFP-positive cells after pCBASce transfection are presumably derived from the recombination of the GFP gene in the chromosome, and reach a maximum level at 5 days posttransfection. GFP-positive cells after pNZE-CAG transfection are derived from the transient expression of the plasmid GFP gene, and reach a maximum level at 3 days posttransfection. (The number of transiently GFP-positive cells at 3 days is approximately 3-fold higher than at 5 days.)
ND, not determined.

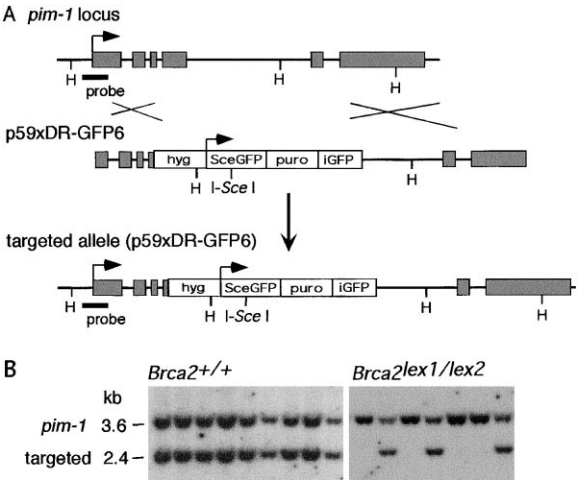

Figure 3. ES Cells with a *Brca2* Exon 27 Deletion Have Reduced Gene Targeting

(A) The *pim1* genomic locus and the p59xDR-GFP6 vector gene targeted to the *pim1* locus. Clones that are gene targeted at *pim1* are efficiently selected in hygromycin, since the hyg^R gene is promoterless in the targeting vector, but is expressed from the *pim1* promoter upon homologous integration. In p59xDR-GFP6, *SceGFP* and *iGFP* are in the same orientation as the *pim1*- and *hyg*-coding sequences. Not shown is the p59xDR-GFP4 vector, in which *SceGFP* and *iGFP* are in the opposite orientation, due to insertion of the entire DR-GFP substrate in the reverse direction into the p59x *pim*–targeting vector. H, HincII sites.

(B) Southern blot analysis of hyg^R clones derived from $Brca2^{+/+}$ and $Brca2^{lex1/lex2}$ ES cells transfected with a p59xDR-GFP-targeting vector. DNA from individually expanded clones was digested with HincII and hybridized with the *pim1* probe shown in (A).

cellular hygromycin resistance is dependent on either homologous targeting to the *pim1* locus or a fortuitous nonhomologous integration adjacent to random promoter sequences.

Linearized p59xDR-GFP6- and p59xDR-GFP4-targeting vectors, which contain DR-GFP in the forward (Figure 3A) or reverse orientation (not shown), respectively, relative to the *pim1* locus, were electroporated into $Brca2^{+/+}$ and $Brca2^{lex1/lex2}$ ES cells, and hyg^R colonies were selected. Genomic DNA from individual hyg^R clones was examined by Southern blotting to determine which clones had undergone gene targeting (Figure 3B). Efficient gene targeting was observed with both targeting vectors in the wild-type ES cells, with 97% of hyg^R clones correctly targeted (139 targeted clones/144 total). The remaining clones were derived from fortuitous random integrations of the targeting vectors in which the *hyg* gene could be expressed. Homologous integrations were also detected in the $Brca2^{lex1/lex2}$ ES cells (64 targeted clones/121 total), but at an approximately 1.8-fold lower frequency. This diminished ability to gene target is suggestive of a homologous recombination defect in cells that are mutated for the *Brca2* gene.

Impaired HDR of a Chromosomal DSB by Gene Conversion in *Brca2*-Deficient ES Cells

Homologous integration of the DR-GFP substrate at the *pim1* locus allows us to examine the ability of cells to repair a DSB by gene conversion at a specific chromosome site. To analyze HDR in the ES cell lines, several of the targeted $Brca2^{+/+}$ and $Brca2^{lex1/lex2}$ clones were transiently transfected with the I-SceI expression vector (pCBASce), the GFP expression vector (pCAG-NZE), or a negative control DNA. Electroporated cells were typically examined 48 hr later by flow cytometry. Results from one set of experiments are shown in Figure 4A. GFP-positive cells were undetected or rarely detected ($<0.01\%$) in either the wild-type or $Brca2^{lex1/lex2}$ clones transfected with the negative control DNA, indicating that spontaneous intrachromosomal gene conversion is rare. Following transfection with pCBASce, GFP-positive cells were readily detected in the $Brca2^{+/+}$ cells. The percentage of GFP-positive cells increased from 24 to 40 hr, where it then remained stable at approximately 3% of the electroporated cells.

In the $Brca2^{lex1/lex2}$ clones, recombination was also induced by I-SceI expression; however, the number of recombinants was lower relative to the $Brca2^{+/+}$ clones, at approximately 0.5% to 0.6% in this experiment (Figure 4A). A similar reduction in the recovery of recombinants was found for both orientations of the DR-GFP substrate. Over several experiments, the average reduction in recombination for the $Brca2^{lex1/lex2}$ clones, as compared with the $Brca2^{+/+}$ clones, was 5- to 6-fold. In control transfections of the GFP expression vector, equal numbers of GFP-positive cells were observed for both cell lines (data not shown), indicating that transfection efficiency is not compromised in the $Brca2^{lex1/lex2}$ cell lines.

The DR-GFP repair substrate was specifically designed to detect DSB repair by gene conversion. To confirm that GFP expression in cells was dependent on gene conversion, physical analysis was performed on the repair substrate in GFP-positive cells. $Brca2^{+/+}$ and $Brca2^{lex1/lex2}$ cells were transiently transfected with the I-SceI expression vector and then sorted by flow cytometry into GFP-positive and GFP-negative populations.

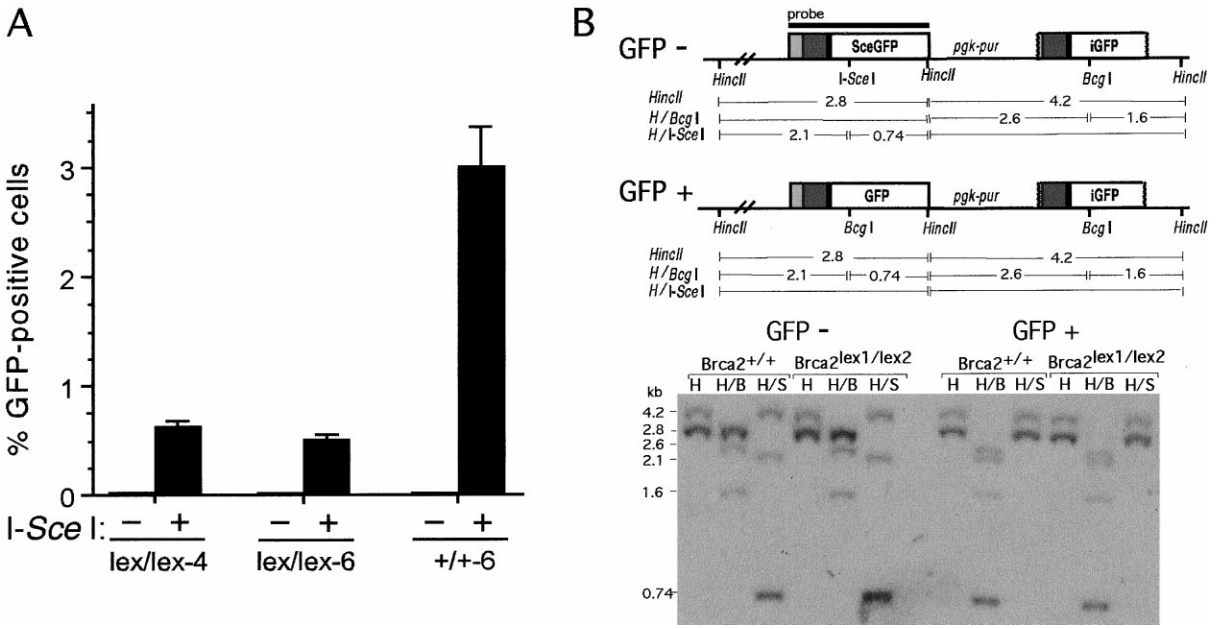

Figure 4. ES Cells with a *Brca2* Exon 27 Deletion Have Reduced HDR of DSBs

(A) Gene conversion within the DR-GFP substrate as deduced from the percentage of GFP-positive cells. Results from targeted $Brca2^{lex1/lex2}$ and $Brca2^{+/+}$ ES cell lines are shown from a representative experiment. Bars not detectable above the x axis depict the infrequent occurrence of GFP-positive cells after transfection with negative control DNA, whereas the visible black bars depict the percent GFP-positive cells following transfection of the I-SceI expression vector. I-SceI expression strongly induces the number of GFP-positive $Brca2^{+/+}$ cells, indicating robust DSB repair by gene conversion; however, $Brca2^{lex1/lex2}$ cells have 5- to 6-fold fewer GFP-positive cells, indicating impaired HDR of a DSB by gene conversion. In this analysis, at least seven independent clones from each mutant genotype were analyzed. lex/lex-4 indicates $Brca2^{lex1/lex2}$ cells targeted with the p59xDR-GFP4 vector; lex/lex-6 and +/+-6 indicate $Brca2^{lex1/lex2}$ and wild-type cells, respectively, targeted with the p59xDR-GFP6 vector. Error bars indicate the SEM.

(B) Physical confirmation of HDR of the I-SceI-induced DSB. After DSB induction, $Brca2^{+/+}$ and $Brca2^{lex1/lex2}$ cells were sorted based on GFP expression, and genomic DNA extracted from each of the sorted pools was analyzed by Southern blotting. Cells that do not express GFP after I-SceI expression (GFP−) retain the I-SceI site in the DR-GFP substrate. By contrast, cells that express GFP after I-SceI expression (GFP+) have repaired the I-SceI-induced DSB by gene conversion with the downstream *iGFP* gene fragment to restore the BcgI site. (Note: As this is a population analysis, cells present in the GFP-negative population at low frequency that have repaired the I-SceI site by other mechanisms would not be detected in this analysis.) H, HincII; B, BcgI; S, I-SceI.

After expansion, genomic DNA was extracted from each of the sorted pools and analyzed by Southern blotting. Whereas GPF-negative cells retained the I-SceI site in the DR-GFP substrate, GFP-positive cells had lost the site (Figure 4B). The I-SceI site in the GFP-positive cells was repaired with restoration of the BcgI site, providing conclusive evidence of DSB repair by gene conversion with the downstream *iGFP* gene fragment. This was apparent in GFP-positive populations derived from either the $Brca2^{+/+}$ or $Brca2^{lex1/lex2}$ cells, indicating that the GFP-positive cells in the $Brca2^{lex1/lex2}$ mutant were also derived by gene conversion rather than by a novel type of repair.

In Vivo Interaction of Brca2 with Rad51

The CAPAN-1 cell line, which harbors a BRCA2-truncating mutation within the BRC repeats (Figure 1A), rarely exhibited cellular green fluorescence following induction of a chromosome break, indicating a profound defect in HDR in these cell lines. However, the $Brca2^{lex1/lex2}$ cells, in which the truncating mutations are well removed from the BRC repeats, had a smaller reduction in HDR. Although it is difficult to directly compare the magnitude of a gene conversion defect in different cell types, it would seem probable that this difference is related to the extent of Brca2 truncation and the ability of the truncated proteins to be expressed and to interact with Rad51. A truncated BRCA2 protein has been demonstrated to be expressed in CAPAN-1 cells, although reports vary on the extent of expression (Marmorstein et al., 1998; Su et al., 1998). The truncated protein interacts with Rad51 by coimmunoprecipitation (Chen et al., 1998a; Marmorstein et al., 1998); however, the Rad51–BRCA2 complexes may be reduced (Marmorstein et al., 1998), and, significantly, the truncated protein is primarily detected in cytoplasmic extracts (Spain et al., 1999). Consistent with this, a nuclear localization signal was recently identified at the C terminus of the human BRCA2 protein, which is deleted in the truncated BRCA2 protein in CAPAN-1 cells (Spain et al., 1999; Yano et al., 2000).

Truncation of the mouse protein could likewise affect protein stability or localization. Although a nuclear localization signal for the mouse Brca2 protein has not been functionally determined, comparison of the mouse and human proteins shows significant sequence conservation in this region of the protein, which is encoded by exon 27 and therefore deleted in the $Brca2^{lex}$ alleles. To evaluate the stability and localization of the truncated mouse protein, Western blotting of extracts from the *Brca2* mutant cell line was performed with antibodies

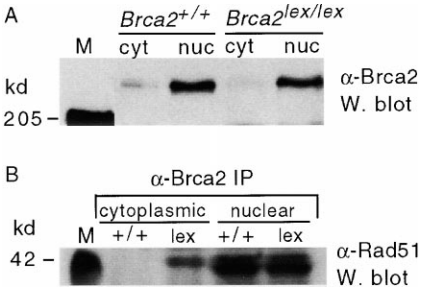

Figure 5. Brca2 Expression and Rad51–Brca2 Interaction in the *Brca2*$^{lex1/lex2}$ ES Cells

(A) Western blot analysis of cytoplasmic and nuclear extracts using an antibody directed against the BRCA2 protein. In both *Brca2*$^{+/+}$ and *Brca2*$^{lex1/lex2}$ ES cells, Brca2 is primarily nuclear. Immunoblotting was performed with the anti-BRCA2 Ab-2 antibody.

(B) Immunoprecipitation of nuclear and cytoplasmic extracts using an anti-BRCA2 antibody followed by Western blot analysis using an anti-Rad51 antibody as a probe. Nuclear coimmunoprecipitates are similar in both *Brca2*$^{+/+}$ and *Brca2*$^{lex1/lex2}$ ES cells, although *Brca2*$^{lex1/lex2}$ also shows a reproducible signal in the cytoplasm, albeit significantly lower than the nuclear signal. +/+, extracts from *Brca2*$^{+/+}$ cells; lex, extracts from *Brca2*$^{lex1/lex2}$ cells.

directed against Brca2. Fractionated extracts from the *Brca2*$^{lex1/lex2}$ ES cells demonstrated a robust signal that was predominantly localized to the nucleus (Figure 5A), despite deletion of the presumed nuclear localization signal. Thus, it is likely that there is another, as yet unidentified, motif in the mouse protein that can confer nuclear localization. In both wild-type and mutant cells, a small amount of the protein was apparent in the cytoplasmic extract.

Since Western blotting indicated that Brca2 protein was present in the *Brca2*$^{lex1/lex2}$ cells, further biochemical analysis was performed to determine whether the protein interacted with Rad51. Western blot analysis indicated that Rad51 levels were similar in *Brca2*$^{+/+}$ and *Brca2*$^{lex1/lex2}$ cells, and that it was distributed in both the nucleus and cytoplasm (data not shown), as has been found in human cells (Davies et al., 2001 [this issue of Molecular Cell]). Nuclear and cytoplasmic extracts derived from *Brca2*$^{+/+}$ and *Brca2*$^{lex1/lex2}$ cells were immunoprecipitated with the anti-Brca2 antibody and immunoblotted with an anti-Rad51 antibody (Figure 5B). Rad51–Brca2 interactions in the nucleus appeared unperturbed in the *Brca2*$^{lex1/lex2}$ cells, although some signal was also detected in the cytoplasm of these cells. Therefore, despite the loss of the C-terminal Rad51 interaction domain in the *Brca2*$^{lex1/lex2}$ cells, a deficiency in Rad51–Brca2 interaction is not apparent.

Discussion

These results directly demonstrate a role for BRCA2 in homologous recombination, specifically in efficient HDR of DNA damage. Impaired HDR of DSBs is observed in human cells that contain a common mutation in families at risk for breast cancer, as well as in a mouse cell line containing a targeted mutation. The magnitude of the defect in the human CAPAN-1 cells is >100-fold as compared with other human cell lines, whereas in the *Brca2*$^{lex1/lex2}$ ES cells, HDR is reduced 5- to 6-fold relative to wild-type ES cells. Thus, the severity of the defect was significantly greater in cells that express a highly truncated BRCA2 protein than in cells in which only the most C-terminal Rad51-interacting domain is perturbed. Gene targeting as assayed in the mouse cells was also reduced.

Although *BRCA1* and *BRCA2* show no homology, the two genes share several characteristics aside from a predisposition to breast and ovarian cancer when mutated. For example, disruptions of *Brca1* and *Brca2* in the mouse lead to early embryonic lethality, and both proteins colocalize to nuclear foci with Rad51. In addition to *BRCA2* mutant cell lines, we have previously examined homologous recombination in ES cells containing a *Brca1* hypomorphic allele (Moynahan et al., 1999). The magnitude of the HDR defect in the *Brca1* mutant cells was similar to that in the *Brca2*$^{lex1/lex2}$ cells. However, the gene-targeting defect was much more severe, approximately 20-fold in the *Brca1* mutant compared to less than 2-fold in the *Brca2* mutant. This suggests that, although these two proteins are both involved in homologous recombination, they have divergent contributions to different recombination pathways.

The HDR defect in the BRCA2-deficient cells is consistent with their hypersensitivity to ionizing radiation and other damaging agents that produce DSBs (Abbott et al., 1998; Chen et al., 1998b; Morimatsu et al., 1998). CAPAN-1 cells have also been found to be defective for ionizing radiation–induced foci of Rad51 (Rad51-IRIF), despite the ability of the truncated protein to interact with Rad51 (Marmorstein et al., 1998; Yuan et al., 1999). This is likely due to the cytoplasmic location of the BRCA2 and Rad51 proteins in these cells (Spain et al., 1999; Davies et al., 2001). The significance of Rad51-IRIF for DSB repair is unknown. However, in addition to BRCA2 mutants, three other cell lines that have defective Rad51-IRIF also have HDR defects. These cell lines are mutant for Brca1 (Moynahan et al., 1999; Bhattacharyya et al., 2000), Rad54 (Tan et al., 1999; Dronkert et al., 2000), and the Rad51-related protein XRCC3 (Bishop et al., 1998; Pierce et al., 1999). Although it is possible that BRCA2 and these other three proteins are each directly required for the physical assembly of Rad51 into nuclear foci, an alternative is that disruptions in HDR per se cause defects in Rad51-IRIF.

Null mutations of *Brca2*, like *Rad51* and *Brca1*, confer an early embryonic lethality in the mouse and an inability to recover viable cell lines (Hakem et al., 1996; Lim and Hasty, 1996; Liu et al., 1996; Tsuzuki et al., 1996; Ludwig et al., 1997; Sharan et al., 1997; Suzuki et al., 1997; Shen et al., 1998). *Brca2* hypomorphic alleles that allow animal and cell survival preserve at least a few BRC domains (Connor et al., 1997; Friedman et al., 1998; Morimatsu et al., 1998). Formally, it is possible that viability is unrelated to recombination; however, enough residual recombination activity may be preserved in these truncation mutants to permit survival. Consistent with this, our DSB assay detects rare GFP-positive cells following DSB induction in the CAPAN-1 cells, indicating that a limited amount of HDR is still possible.

Peptides encoding the third or fourth BRC repeat (BRC3 or BRC4) have recently been shown to disrupt Rad51 nucleoprotein filament formation (Davies et al.,

2001). Additionally, overexpression of BRC4 confers radiation sensitivity to cell lines containing wild-type BRCA2; significantly, a point mutation in the small BRC4 peptide, which has been observed to be a cancer-conferring mutation, abrogates the radiation hypersensitivity (Chen et al., 1999). The decrease in HDR we have observed can be due to improper sequestration of Rad51 by stably expressed products that retain BRC repeats, as for the CAPAN-1 cells (Davies et al., 2001). Significantly, impaired HDR repair is found in the *Brca2*$^{lex1/lex2}$ cells even though Rad51–Brca2 interaction in the nucleus is largely intact. This implies that the truncated Brca2 protein may have a more subtle defect in Rad51 interaction or localization not obvious by coimmunoprecipitation, or that the extreme C terminus plays an additional role in recombination.

Some mutation carriers, such as those with the 6174delT mutation, are expected to express a truncated BRCA2 protein, which like wild-type BRCA2 can interact with Rad51. As yet, it is unknown whether truncated BRCA2, which retains some interaction with Rad51, diminishes HDR in the presence of wild-type BRCA2. A heterozygote phenotype for viability or tumorigenesis has not been reported in mice with targeted *Brca2* alleles, and thus far human tumors derived from *BRCA2* mutation carriers consistently reveal loss of the wild-type allele. However, more subtle changes, such as in breast and ovary morphology, have been described in mice heterozygous for either *Brca1* or *Brca2* mutations, and these changes may be exacerbated by carcinogen exposure (Bennett et al., 2000). As well, it has been reported that cells from *BRCA1* and *BRCA2* mutation carriers are more radiosensitive than cells from wild-type individuals (Foray et al., 1999). Given the sensitivity and technical ease of the DSB repair assay used in this study, the efficiency of HDR in carriers of various *BRCA2* mutations can be explored.

The recombination construct used in this system detects one type of HDR, specifically gene conversion unaccompanied by crossing-over. Noncrossover gene conversion is a common HDR pathway in mammalian cells for the repair of DSBs and employs sister chromatids, homologs, and heterologs, with the primary template for HDR being the sister chromatid (Moynahan and Jasin, 1997; Liang et al., 1998; Richardson et al., 1998; Johnson et al., 1999; Johnson and Jasin, 2000). The DR-GFP substrate, by analogy to other substrates, is believed to provide a measure of both unequal sister chromatid and intrachromatid recombination (Pierce et al., 1999; Johnson and Jasin, 2000), which leads us to propose that BRCA2 has a general role in sister chromatid recombination in proliferating cells. Consistent with a role for BRCA2 following DNA replication, mRNA expression peaks at the G1/S boundary (Rajan et al., 1996; Tashiro et al., 1996; Vaughn et al., 1996), with protein levels increasing as cells enter S phase (Bertwistle et al., 1997; Su et al., 1998). Rad51 shows a similar cell cycle–dependent expression (Yamamoto et al., 1996). Recent studies in *E. coli* have demonstrated that the main function of homologous recombination under normal growth conditions is to restart stalled replication forks (Cox et al., 2000). Direct evidence for a similar role in mammalian cells is not available; however, the lethality of *Rad51*, *Brca1,* and *Brca2* null mutations and the inhibition of cell division upon *Rad51* downregulation (Taki et al., 1996) support such a role for homologous recombination in mammalian cells.

In addition to homologous recombination, DSBs can also be repaired efficiently in mammalian cells by nonhomologous mechanisms (Liang et al., 1998). Both of these repair pathways are implicated in the maintenance of genetic integrity, as cells with homologous or nonhomologous repair defects exhibit gross chromosomal rearrangements (Shen et al., 1998; Cui et al., 1999; Karanjawala et al., 1999; Difilippantonio et al., 2000; Gao et al., 2000), including cells with hypomorphic *Brca2* alleles (Patel et al., 1998; Lee et al., 1999; Yu et al., 2000). That the HDR deficiency is responsible for the genomic instability of Brca2-deficient cells is supported by their apparent proficiency in nonhomologous repair, as determined by V(D)J recombination (Patel et al., 1998) and in vitro end-joining assays (Yu et al., 2000). Although the precise etiology of gross chromosomal rearrangements is not understood, translocations were recently shown to occur between two broken chromosomes in normal cells (Richardson and Jasin, 2000). The translocations arose by nonhomologous end-joining and simple annealing at homologous repeats, but not by gene conversion repair (Richardson and Jasin, 2000). It is possible, therefore, that when HDR is disrupted, DSBs usually repaired by gene conversion are instead repaired by other mechanisms that are more prone to giving rise to translocations and other gross chromosomal rearrangements.

The cellular response to chromosome breaks, including which pathway to repair, may be determined by the cell cycle phase, differentiation status of the cell, and the tissue type (Gao et al., 1998; Takata et al., 1998; Essers et al., 2000). Cells that have exited the cell cycle may be more dependent on nonhomologous repair, whereas cells that are self-renewing, such as during embryogenesis and in some adult tissues, may be more dependent on HDR to repair DSBs that arise during cell division. Whether the tissue specificity seen in hereditary breast cancer predisposition is attributable to a dependence on HDR during key developmental periods or during renewal of cycling epithelial stem cells is an important area for future investigation.

BRCA2, unlike BRCA1, has relatively few alternative hypotheses as to its tumor suppressor function (Welcsh et al., 2000). The striking chromosomal instability phenotype that accompanies HDR deficiencies is a hallmark of human solid tumors, including *BRCA2*-associated tumors (Tirkkonen et al., 1997). The profound defect in HDR of chromosome breaks in *BRCA2* mutant cells confirms a caretaker function for BRCA2 in protecting genomic integrity through efficient repair of DNA damage by homologous recombination.

Experimental Procedures

DNA Manipulations

The p59xDR-GFP6- and p59xDR-GFP4 *pim1*–targeting vectors were constructed by modifying the previously described gene-targeting vector, p59 (te Riele et al., 1990), to contain XhoI sites flanking the targeting arms (p59x) and the DR-GFP recombination substrate (Pierce et al., 1999). The phHPRT-DR-GFP plasmid was digested with AvrII, and the ends were filled in by Klenow polymerase, followed by digestion with SspI. The 6.7 kb fragment containing DR-

GFP was cloned into the p59x-targeting vector at a unique SmaI site 30 bp downstream of the *hyg*-coding sequences. Constructs containing DR-GFP in both the forward and reverse orientations relative to the *hyg* gene were created (p59DR-GFP6 and p59DR-GFP4, respectively). The targeting fragments were obtained by XhoI digestion.

Cell Transfections and Southern Analysis

For stable transfection, CAPAN-1 cells were electroporated at 800 V/3 μF with 75 μg of the SacI/KpnI fragment from phHPRT-DR-GFP, followed by selection after 48 hr in 0.4 μg/ml puromycin. Puromycin-resistant clones were selected and expanded 21 to 30 days later. Southern blots of genomic DNA from these clones were probed with a radiolabeled 1.4 kb HpaI-NarI GFP fragment from pNZE-CAG. CAPAN-1 clones 4, 5, 8, 11, and 23 were confirmed using PstI, HindIII, BglII, and SpeI analysis to have integrated an intact DR-GFP fragment. Overall, 13% of the analyzed puromycin-resistant CAPAN-1 clones had randomly integrated an intact DR-GFP repair substrate. The CAPAN-1 6174delT mutation was verified by DNA sequencing.

For gene targeting, ES cells were electroporated with 75 μg of linear targeting fragment from p59xDR-GFP, followed by selection after 48 hr in 110 μg/ml hygromycin and 1.0 μg/ml puromycin. For DSB repair assays, actively growing cells were electroporated at 250 V/960 μF with 30 to 50 μg of pCBASce (Richardson et al., 1998), mock DNA, or pNZE-CAG (Pierce et al., 1999), and plated in nonselective media. Cells were trypsinized at the indicated times and analyzed by flow cytometry. Data were analyzed with Lysis software.

For physical confirmation of HDR, 1×10^8 ES cells were transfected with 100 μg of pCBASce, and 48 hr afterwards, transfection cells were sorted based on GFP expression. Collections of GFP-negative and GFP-positive cells were expanded. Digested genomic DNA was probed with the 1.4 kb GFP fragment as depicted in Figure 4B.

Protein Manipulations

Cytoplasmic and nuclear fractions were prepared in buffers A and C and the nuclear fraction was dialyzed in buffer D, as described (Lee et al., 1994). Total protein content was determined by Bio-Rad DC protein assay. For Western blot analysis of Brca2 protein, 100 μg of fractionated lysate was electrophoresed by 4.5% SDS-PAGE and probed with an anti-BRCA2 Ab-2 antibody (Oncogene Research). For coimmunoprecipitation, 1 mg of cytoplasmic extract and 500 μg of nuclear extract were immunoprecipitated with 1 mg of an anti-BRCA2 antibody and separated by 10% SDS-PAGE. The probe was an anti-Rad51 antibody (a gift of Steve West).

Acknowledgments

We thank Paul Hasty and Lexicon Genetics for the gift of the *Brca2*$^{lex1/lex2}$ cells. This work was supported by the Department of the Army (DAMD17-98-1-8334) and the National Institutes of Health Specialized Program of Research Excellence in breast cancer (1P50CA68425).

Received August 24, 2000; revised November 30, 2000.

References

Abbott, D.W., Freeman, M.L., and Holt, J.T. (1998). Double-strand break repair deficiency and radiation sensitivity in BRCA2 mutant cancer cells. J. Natl. Cancer Inst. *90*, 978–985.

Abbott, D.W., Thompson, M.E., Robinson-Benion, C., Tomlinson, G., Jensen, R.A., and Holt, J.T. (1999). BRCA1 expression restores radiation resistance in BRCA1-defective cancer cells through enhancement of transcription-coupled DNA repair. J. Biol. Chem. *274*, 18808–18812.

Bennett, L.M., McAllister, K.A., Malphurs, J., Ward, T., Collins, N.K., Seely, J.C., Gowen, L.C., Koller, B.H., Davis, B.J., and Wiseman, R.W. (2000). Mice heterozygous for a Brca1 or Brca2 mutation display distinct mammary gland and ovarian phenotypes in response to diethylstilbestrol. Cancer Res. *60*, 3461–3469.

Bertwistle, D., Swift, S., Marston, N.J., Jackson, L.E., Crossland, S., Crompton, M.R., Marshall, C.J., and Ashworth, A. (1997). Nuclear location and cell cycle regulation of the BRCA2 protein. Cancer Res. *57*, 5485–5488.

Bhattacharyya, A., Ear, U.S., Koller, B.H., Weichselbaum, R.R., and Bishop, D.K. (2000). The breast cancer-susceptibility gene BRCA1 is required for subnuclear assembly of Rad51 and survival following treatment with the DNA crosslinking agent cisplatin. J. Biol. Chem. *275*, 23899–23903.

Bishop, D.K., Ear, U., Bhattacharyya, A., Calderone, C., Beckett, M., Weichselbaum, R.R., and Shinohara, A. (1998). Xrcc3 is required for assembly of Rad51 complexes in vivo. J. Biol. Chem. *273*, 21482–21488.

Chen, J., Silver, D.P., Walpita, D., Cantor, S.B., Gazdar, A.F., Tomlinson, G., Couch, F.J., Weber, B.L., Ashley, T., Livingston, D.M., and Scully, R. (1998a). Stable interaction between the products of the BRCA1 and BRCA2 tumor suppressor genes in mitotic and meiotic cells. Mol. Cell *2*, 317–328.

Chen, P.L., Chen, C.F., Chen, Y., Xiao, J., Sharp, Z.D., and Lee, W.H. (1998b). The BRC repeats in BRCA2 are critical for RAD51 binding and resistance to methyl methanesulfonate treatment. Proc. Natl. Acad. Sci. USA *95*, 5287–5292.

Chen, C.F., Chen, P.L., Zhong, Q., Sharp, Z.D., and Lee, W.H. (1999). Expression of BRC repeats in breast cancer cells disrupts the BRCA2-Rad51 complex and leads to radiation hypersensitivity and loss of G(2)/M checkpoint control. J. Biol. Chem. *274*, 32931–32935.

Connor, F., Bertwistle, D., Mee, P.J., Ross, G.M., Swift, S., Grigorieva, E., Tybulewicz, V.L., and Ashworth, A. (1997). Tumorigenesis and a DNA repair defect in mice with a truncating Brca2 mutation. Nat. Genet. *17*, 423–430.

Cox, M.M. (1999). Recombinational DNA repair in bacteria and the RecA protein. Prog. Nucleic Acid Res. Mol. Biol. *63*, 311–366.

Cox, M.M., Goodman, M.F., Kreuzer, K.N., Sherratt, D.J., Sandler, S.J., and Marians, K.J. (2000). The importance of repairing stalled replication forks. Nature *404*, 37–41.

Cui, X., Brenneman, M., Meyne, J., Oshimura, M., Goodwin, E.H., and Chen, D.J. (1999). The XRCC2 and XRCC3 repair genes are required for chromosome stability in mammalian cells. Mutat. Res. *434*, 75–88.

Davies, A.A., Masson, J.-Y., McIlwraith, M.J., Stasiak, A.Z., Stasiak, A., Venkitaraman, A.R., and West, S.C. BRCA2 controls the RAD51 DNA repair protein. Mol. Cell *7*, this issue, 273–282.

Difilippantonio, M.J., Zhu, J., Chen, H.T., Meffre, E., Nussenzweig, M.C., Max, E.E., Ried, T., and Nussenzweig, A. (2000). DNA repair protein Ku80 suppresses chromosomal aberrations and malignant transformation. Nature *404*, 510–514.

Dronkert, M.L., Beverloo, H.B., Johnson, R.D., Hoeijmakers, J.H., Jasin, M., and Kanaar, R. (2000). Mouse RAD54 affects DNA double-strand break repair and sister chromatid exchange. Mol. Cell. Biol. *20*, 3147–3156.

Essers, J., Hendriks, R.W., Swagemakers, S.M., Troelstra, C., de Wit, J., Bootsma, D., Hoeijmakers, J.H., and Kanaar, R. (1997). Disruption of mouse RAD54 reduces ionizing radiation resistance and homologous recombination. Cell *89*, 195–204.

Essers, J., van Steeg, H., de Wit, J., Swagemakers, S.M., Vermeij, M., Hoeijmakers, J.H., and Kanaar, R. (2000). Homologous and non-homologous recombination differentially affect DNA damage repair in mice. EMBO J. *19*, 1703–1710.

Foray, N., Randrianarison, V., Marot, D., Perricaudet, M., Lenoir, G., and Feunteun, J. (1999). γ-rays-induced death of human cells carrying mutations of BRCA1 or BRCA2. Oncogene *18*, 7334–7342.

Friedman, L.S., Thistlethwaite, F.C., Patel, K.J., Yu, V.P., Lee, H., Venkitaraman, A.R., Abel, K.J., Carlton, M.B., Hunter, S.M., Colledge, W.H., et al. (1998). Thymic lymphomas in mice with a truncating mutation in Brca2. Cancer Res. *58*, 1338–1343.

Gao, Y., Chaudhuri, J., Zhu, C., Davidson, L., Weaver, D.T., and Alt, F.W. (1998). A targeted DNA-PKcs-null mutation reveals DNA-PK-independent functions for KU in V(D)J recombination. Immunity *9*, 367–376.

Gao, Y., Ferguson, D.O., Xie, W., Manis, J.P., Sekiguchi, J., Frank,

K.M., Chaudhuri, J., Horner, J., DePinho, R.A., and Alt, F.W. (2000). Interplay of p53 and DNA-repair protein XRCC4 in tumorigenesis, genomic stability and development. Nature *404*, 897–900.

Goggins, M., Schutte, M., Lu, J., Moskaluk, C.A., Weinstein, C.L., Petersen, G.M., Yeo, C.J., Jackson, C.E., Lynch, H.T., Hruban, R.H., and Kern, S.E. (1996). Germline BRCA2 gene mutations in patients with apparently sporadic pancreatic carcinomas. Cancer Res. *56*, 5360–5364.

Gowen, L.C., Avrutskaya, A.V., Latour, A.M., Koller, B.H., and Leadon, S.A. (1998). BRCA1 required for transcription-coupled repair of oxidative DNA damage. Science *281*, 1009–1012.

Hakem, R., de la Pompa, J.L., Sirard, C., Mo, R., Woo, M., Hakem, A., Wakeham, A., Potter, J., Reitmair, A., Billia, F., et al. (1996). The tumor suppressor gene *Brca1* is required for embryonic cellular proliferation in the mouse. Cell *85*, 1009–1023.

Jeggo, P.A. (1998). DNA breakage and repair. Adv. Genet. *38*, 185–218.

Johnson, R.D., and Jasin, M. (2000). Sister chromatid gene conversion is a prominent double-strand break repair pathway in mammalian cells. EMBO J. *19*, 3398–3407.

Johnson, R.D., Liu, N., and Jasin, M. (1999). Mammalian XRCC2 promotes the repair of DNA double-strand breaks by homologous recombination. Nature *401*, 397–399.

Karanjawala, Z.E., Grawunder, U., Hsieh, C.L., and Lieber, M.R. (1999). The nonhomologous DNA end joining pathway is important for chromosome stability in primary fibroblasts. Curr. Biol. *9*, 1501–1504.

Lee, H., Trainer, A.H., Friedman, L.S., Thistlethwaite, F.C., Evans, M.J., Ponder, B.A., and Venkitaraman, A.R. (1999). Mitotic checkpoint inactivation fosters transformation in cells lacking the breast cancer susceptibility gene, Brca2. Mol. Cell *4*, 1–10.

Lee, K.A.W., Zerivitz, K., and Akusjarvl, G. (1994). Small-scale preparation of nuclear extracts from mammalian cells. In Cell Biology: A Laboratory Handbook, vol. 1, J.E. Celis, ed. (San Diego, CA: Academic Press), pp. 668–670.

Liang, F., Han, M., Romanienko, P.J., and Jasin, M. (1998). Homology-directed repair is a major double-strand break repair pathway in mammalian cells. Proc. Natl. Acad. Sci. USA *95*, 5172–5177.

Lim, D.-S., and Hasty, P. (1996). A mutation in mouse rad51 results in an early embryonic lethal that is suppressed by a mutation in p53. Mol. Cell. Biol. *16*, 7133–7143.

Liu, C.Y., Fleskin-Nikitin, A., Li, S., Zeng, Y., and Lee, W.H. (1996). Inactivation of the mouse BRCA1 gene leads to failure in the morphogenesis of the egg cylinder in early postimplantation development. Genes Dev. *10*, 1835–1843.

Ludwig, T., Chapman, D.L., Papaioannou, V.E., and Efstratiadis, A. (1997). Targeted mutations of breast cancer susceptibility gene homologs in mice: lethal phenotypes of Brca1, Brca2, Brca1/Brca2, Brca1/p53, and Brca2/p53 nullizygous embryos. Genes Dev. *11*, 1226–1241.

Marmorstein, L.Y., Ouchi, T., and Aaronson, S.A. (1998). The BRCA2 gene product functionally interacts with p53 and RAD51. Proc. Natl. Acad. Sci. USA *95*, 13869–13874.

Mizuta, R., LaSalle, J.M., Cheng, H.L., Shinohara, A., Ogawa, H., Copeland, N., Jenkins, N.A., Lalande, M., and Alt, F.W. (1997). RAB22 and RAB163/mouse BRCA2: proteins that specifically interact with the RAD51 protein. Proc. Natl. Acad. Sci. USA *94*, 6927–6932.

Morimatsu, M., Donoho, G., and Hasty, P. (1998). Cells deleted for Brca2 COOH terminus exhibit hypersensitivity to γ-radiation and premature senescence. Cancer Res. *58*, 3441–3447.

Moynahan, M.E., and Jasin, M. (1997). Loss of heterozygosity induced by a chromosomal double-strand break. Proc. Natl. Acad. Sci. USA *94*, 8988–8993.

Moynahan, M.E., Chiu, J.W., Koller, B.H., and Jasin, M. (1999). Brca1 controls homology-directed repair. Mol. Cell *4*, 511–518.

Pâques, F., and Haber, J.E. (1999). Multiple pathways of recombination induced by double-strand breaks in *Saccharomyces cerevisiae*. Microbiol. Mol. Biol. Rev. *63*, 349–404.

Patel, K.J., Vu, V.P., Lee, H., Corcoran, A., Thistlethwaite, F.C., Evans, M.J., Colledge, W.H., Friedman, L.S., Ponder, B.A., and Venkitaraman, A.R. (1998). Involvement of Brca2 in DNA repair. Mol. Cell *1*, 347–357.

Pierce, A.J., Johnson, R.D., Thompson, L.H., and Jasin, M. (1999). XRCC3 promotes homology-directed repair of DNA damage in mammalian cells. Genes Dev. *13*, 2633–2638.

Rahman, N., and Stratton, M.R. (1998). The genetics of breast cancer susceptibility. Annu. Rev. Genet. *32*, 95–121.

Rajan, J.V., Wang, M., Marquis, S.T., and Chodosh, L.A. (1996). Brca2 is coordinately regulated with Brca1 during proliferation and differentiation in mammary epithelial cells. Proc. Natl. Acad. Sci. USA *93*, 13078–13083.

Richardson, C., and Jasin, M. (2000). Frequent chromosomal translocations induced by DNA double-strand breaks. Nature *405*, 697–700.

Richardson, C., Moynahan, M.E., and Jasin, M. (1998). Double-strand break repair by interchromosomal recombination: suppression of chromosomal translocations. Genes Dev. *12*, 3831–3842.

Scully, R., Chen, J., Plug, A., Xiao, Y., Weaver, D., Feunteun, J., Ashley, T., and Livingston, D.M. (1997). Association of BRCA1 with Rad51 in mitotic and meiotic cells. Cell *88*, 265–275.

Sharan, S.K., and Bradley, A. (1997). Murine Brca2: sequence, map position, and expression pattern. Genomics *40*, 234–241.

Sharan, S.K., Morimatsu, M., Albrecht, U., Lim, D.-S., Regel, E., Dinh, C., Sands, A., Eichele, G., Hasty, P., and Bradley, A. (1997). Embryonic lethality and radiation hypersensitivity mediated by Rad51 in mice lacking *Brca2*. Nature *386*, 804–810.

Shen, S.X., Weaver, Z., Xu, X., Li, C., Weinstein, M., Chen, L., Guan, X.Y., Ried, T., and Deng, C.X. (1998). A targeted disruption of the murine Brca1 gene causes γ-irradiation hypersensitivity and genetic instability. Oncogene *17*, 3115–3124.

Spain, B.H., Larson, C.J., Shihabuddin, L.S., Gage, F.H., and Verma, I.M. (1999). Truncated BRCA2 is cytoplasmic: implications for cancer-linked mutations. Proc. Natl. Acad. Sci. USA *96*, 13920–13925.

Su, L.K., Wang, S.C., Qi, Y., Luo, W., Hung, M.C., and Lin, S.H. (1998). Characterization of BRCA2: temperature sensitivity of detection and cell-cycle regulated expression. Oncogene *17*, 2377–2381.

Suzuki, A., de la Pompa, J.L., Hakem, R., Elia, A., Yoshida, R., Mo, R., Nishina, H., Chuang, T., Wakeham, A., Itie, A., et al. (1997). Brca2 is required for embryonic cellular proliferation in the mouse. Genes Dev. *11*, 1242–1252.

Takata, M., Sasaki, M.S., Sonoda, E., Morrison, C., Hashimoto, M., Utsumi, H., Yamaguchi-Iwai, Y., Shinohara, A., and Takeda, S. (1998). Homologous recombination and non-homologous end-joining pathways of DNA double-strand break repair have overlapping roles in the maintenance of chromosomal integrity in vertebrate cells. EMBO J. *17*, 5497–5508.

Taki, T., Ohnishi, T., Yamamoto, A., Hiraga, S., Arita, N., Izumoto, S., Hayakawa, T., and Morita, T. (1996). Antisense inhibition of the RAD51 enhances radiosensitivity. Biochem. Biophys. Res. Commun. *223*, 434–438.

Tan, T.L., Essers, J., Citterio, E., Swagemakers, S.M., de Wit, J., Benson, F.E., Hoeijmakers, J.H., and Kanaar, R. (1999). Mouse Rad54 affects DNA conformation and DNA-damage-induced Rad51 foci formation. Curr. Biol. *9*, 325–328.

Tashiro, S., Kotomura, N., Shinohara, A., Tanaka, K., Ueda, K., and Kamada, N. (1996). S phase specific formation of the human Rad51 protein nuclear foci in lymphocytes. Oncogene *12*, 2165–2170.

te Riele, H., Maandag, E.R., Clarke, A., Hooper, M., and Berns, A. (1990). Consecutive inactivation of both alleles of the *pim-1* proto-oncogene by homologous recombination in embryonic stem cells. Nature *348*, 649–651.

Tirkkonen, M., Johannsson, O., Agnarsson, B.A., Olsson, H., Ingvarsson, S., Karhu, R., Tanner, M., Isola, J., Barkardottir, R.B., Borg, A., and Kallioniemi, O.P. (1997). Distinct somatic genetic changes associated with tumor progression in carriers of BRCA1 and BRCA2 germ-line mutations. Cancer Res. *57*, 1222–1227.

Tsuzuki, T., Fujii, Y., Sakumi, K., Tominaga, Y., Nakao, K., Sekiguchi, M., Matsushiro, A., Yoshimura, Y., and Morita, T. (1996). Targeted

disruption of the Rad51 gene leads to lethality in embryonic mice. Proc. Natl. Acad. Sci. USA *93*, 6236–6340.

Vaughn, J.P., Cirisano, F.D., Huper, G., Berchuck, A., Futreal, P.A., Marks, J.R., and Iglehart, J.D. (1996). Cell cycle control of BRCA2. Cancer Res. *56*, 4590–4594.

Welcsh, P.L., Owens, K.N., and King, M.C. (2000). Insights into the functions of BRCA1 and BRCA2. Trends Genet. *16*, 69–74.

Wong, A.K.C., Pero, R., Ormonde, P.A., Tavtigian, S.V., and Bartel, P.L. (1997). RAD51 interacts with the evolutionarily conserved BRC motifs in the human breast cancer susceptibility gene brca2. J. Biol. Chem. *272*, 31941–31944.

Yamamoto, A., Taki, T., Yagi, H., Habu, T., Yoshida, K., Yoshimura, Y., Yamamoto, K., Matsushiro, A., Nishimune, Y., and Morita, T. (1996). Cell cycle-dependent expression of the mouse Rad51 gene in proliferating cells. Mol. Gen. Genet. *251*, 1–12.

Yano, K., Morotomi, K., Saito, H., Kato, M., Matsuo, F., and Miki, Y. (2000). Nuclear localization signals of the BRCA2 protein. Biochem. Biophys. Res. Commun. *270*, 171–175.

Yu, V.P., Koehler, M., Steinlein, C., Schmid, M., Hanakahi, L.A., van Gool, A.J., West, S.C., and Venkitaraman, A.R. (2000). Gross chromosomal rearrangements and genetic exchange between nonhomologous chromosomes following BRCA2 inactivation. Genes Dev. *14*, 1400–1406.

Yuan, S.S., Lee, S.Y., Chen, G., Song, M., Tomlinson, G.E., and Lee, E.Y. (1999). BRCA2 is required for ionizing radiation-induced assembly of Rad51 complex in vivo. Cancer Res. *59*, 3547–3551.